Drug Design, Development and Therapy

Dovepress
Taylor & Francis Group

Open Access Full Text Article

CLINICAL TRIAL REPORT

Pharmacokinetics, Safety and Tolerability of HPP737, a Novel PDE4 Inhibitor, in Healthy Chinese Participants: Phase I Study

Lijun Ye[1], Lin Wang[1], Xuexia Tao[1], Shufan Cai[1], Nengming Lin[1], Yuannian Li[2], Qian Zhu[2], Qinghua Zhu[2], Fei Wang[3]

[1]Clinical Research Center, Affiliated Hangzhou First People's Hospital, School of Medicine, Westlake University, Hangzhou, Zhejiang, People's Republic of China; [2]Clinical Development, Newsoara Biopharma (Shanghai) Co., Ltd., Shanghai, People's Republic of China; [3]Clinical Research Center, The First Affiliated Hospital of Zhejiang Chinese Medical University (Zhejiang Provincial Hospital of Chinese Medicine), Hangzhou, Zhejiang, People's Republic of China

Correspondence: Fei Wang, Clinical Research Center, The First Affiliated Hospital of Zhejiang Chinese Medical University (Zhejiang Provincial Hospital of Chinese Medicine), No. 54 YouDian Road, Shangcheng District, Hangzhou, 310006, People's Republic of China, Email wfgcp0510@163.com

Background and Objective: HPP737, a novel phosphodiesterase 4 (PDE4) inhibitor, was designed to treat chronic obstructive pulmonary disease (COPD). This study aimed to evaluate its pharmacokinetics, safety and tolerability in healthy Chinese participants.

Methods: In this randomized, double-blind, placebo-controlled study, 72 healthy Chinese participants received single ascending doses (SAD: 6, 10, 20, 30 mg) or multiple ascending doses (MAD: 10, 20 mg once daily for 7 days) of HPP737 or placebo under a standardized high-fat breakfast. Primary endpoints included pharmacokinetic parameters and the incidence and severity of adverse events (AEs).

Results: HPP737 exhibited slow absorption (median T_{max} 11–15 h) and a long elimination half-life (~21.2 h), supporting once-daily dosing. The increase in C_{max} and $AUC_{0\text{-}t}$ were slightly less than dose-proportional. Steady-state plasma concentrations were achieved within 3 days after once administration, with moderate accumulation (accumulation ratios: 1.4–2.2). A distinctive dose-dependent reduction in serum uric acid (hypouricemia) was observed, which was asymptomatic and reversible. Treatment-emergent AEs were predominantly mild (Grade 1) and central nervous system (CNS) -related adverse reactions were notably infrequent; no serious AEs or deaths occurred.

Conclusion: HPP737 showed a favorable pharmacokinetics profile suitable for once-daily administration and was well-tolerated in healthy Chinese participants, with a notably low incidence of CNS-related effects—a common limitation of existing PDE4 inhibitors. Collectively, these findings support the continued clinical development of HPP737 as a potential treatment for COPD.

Keywords: PDE4 inhibitor, HPP737, pharmacokinetics, phase I clinical trial, healthy volunteers, tolerability

Introduction

Chronic Obstructive Pulmonary Disease (COPD) imposes a significant public health crisis worldwide. With approximately 213 million prevalent cases and 16.9 million new cases annually,[1,2] COPD ranks as a leading cause of global mortality and disability.[3] In China, the burden is disproportionately high, accounting for nearly a quarter of global cases.[4,5] This immense and growing prevalence, coupled with the substantial economic burden projected to reach trillions of dollars,[6] underscores the urgent need for developing more effective therapeutic agents.

COPD is characterized by persistent respiratory symptoms and incompletely reversible airflow limitation. Chronic inflammation plays a key role in both the onset and progression of the disease.[7] Although mainstay therapies inhaled corticosteroids are widely used, there remains a significant unmet need for therapies that more effectively target the underlying inflammatory processes and alter the disease course. The phosphodiesterase 4 (PDE4) enzyme degrades cyclic adenosine monophosphate (cAMP),[8] a key second messenger that suppresses inflammatory responses. Inhibiting PDE4 in airway smooth muscle increases intracellular cAMP levels, leading to muscle relaxation and modulation of

https://doi.org/10.2147/DDDT.S598997
Received: 27 January 2026
Accepted: 5 May 2026
Published: 19 May 2026

Graphical Abstract

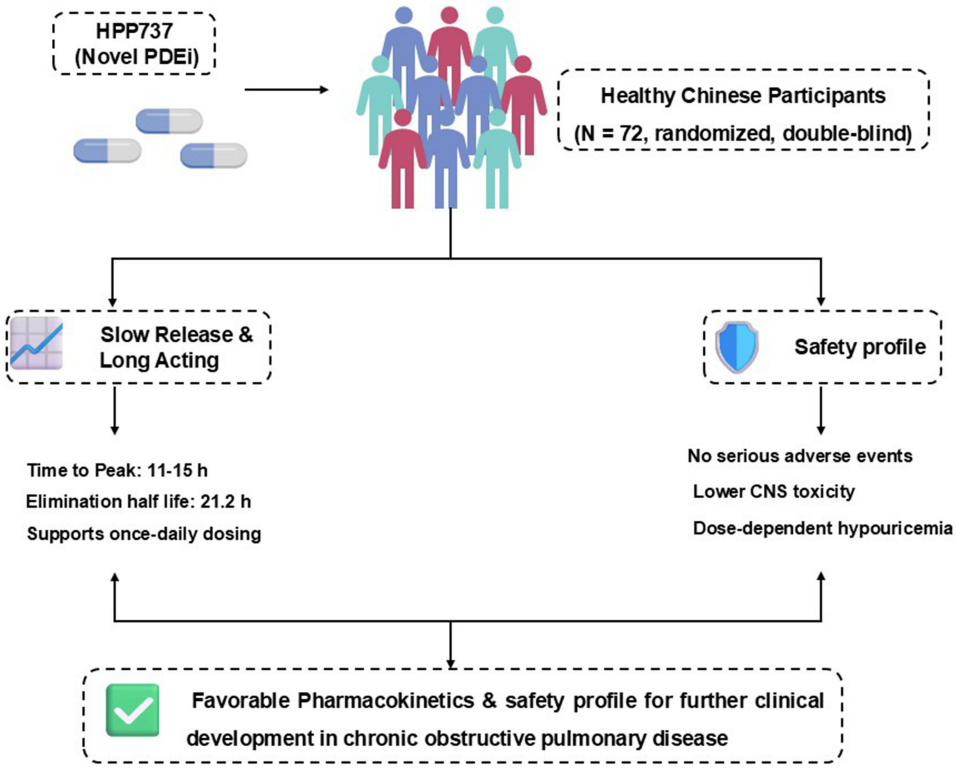

inflammatory cell activity.[9,10] This mechanistic rationale is supported by the clinical approval of the oral PDE4 inhibitor roflumilast for reducing exacerbations in severe COPD.[11–14] However, roflumilast is associated with dose-limiting adverse effects, including most notably psychiatric disorders and a 9.5% incidence of gastrointestinal adverse reactions,[15–21] which often attributed to its central nervous system (CNS) penetration.[22] These tolerability issues frequently lead to treatment discontinuation and have limited the widespread use of roflumilast in clinical practice. Beyond roflumilast, the clinical development landscape of PDE4 inhibitors has seen several candidates, as comprehensively reviewed by Li et al[23] Consequently, developing novel PDE4 inhibitors with improved tolerability profiles, particularly those with reduced CNS permeability, is a key objective in the field.[24]

HPP737 is a novel oral PDE4 inhibitor designed to address this need. Mechanistically distinct from the catecholamine derivatives of roflumilast, HPP737 features a unique quinoline chemical structure. Preclinical data indicate potent PDE4 inhibition coupled with significantly lower CNS permeability, predicting an improved tolerability profile. Notably, roflumilast is rapidly absorbed in rats (time to peak concentration [T_{max}] ~1 hour),[25] whereas HPP737 exhibits slower absorption (median T_{max} 4–8 hours, unpublished data), a feature hypothesized to reduce the risk of CNS-related adverse events by lowering peak plasma concentrations. Preliminary phase I clinical trials in the United States, comprising single ascending dose (SAD: 0.5–20 mg; HPP737-101) and multiple ascending dose (MAD: 3–10 mg once daily for 14 days; HPP737-102) studies in healthy participants, have demonstrated favorable safety and tolerability. To support future regulatory submission and clinical use in China, this study aimed to evaluate the safety, tolerability, and pharmacokinetic characteristics of single and multiple ascending doses of HPP737 in healthy Chinese participants.

Materials and Methods

Study Design

This phase I clinical trial (ClinicalTrials.gov identifier: NCT04714294) was designed to evaluate the pharmacokinetics, safety and tolerability of orally administered HPP737 in healthy Chinese participants. The study featured a randomized, double-blind, placebo-controlled design with SAD and MAD phases. It was conducted in accordance with the Declaration of Helsinki and International Council for Harmonization Clinical Guideline E6 Guideline for Good Clinical Practice. All healthy participants were eligible after signing written informed consent, and the study protocol was reviewed and approved by ethics committee of the Affiliated Hangzhou First People's Hospital.

Study Population

Healthy Chinese male and female volunteers aged 18–45 years were eligible for inclusion. Key inclusion criteria were a body weight of ≥50 kg (males) or ≥45 kg (females) and a body mass index (BMI) between 19 and 24 kg/m^2. Participants of childbearing potential had to agree to use effective contraception for 90 days after the last dose. Major exclusion criteria included: (1) a history of allergies or relevant medical conditions (including malignancy within the past 5 years); (2) clinically significant abnormalities in physical examination, 12-lead electrocardiogram (ECG), or laboratory tests (including positive serology for hepatitis B, hepatitis C, HIV, or syphilis); (3) a history of drug dependence or substance abuse; (4) current smoking or alcohol misuse; (5) participation in another investigational drug or device trial within 3 months prior to enrollment; (6) significant blood loss or transfusion within defined periods prior to screening; and (7) Taking any prescription medications or herbal products within 4 weeks, or any over-to-counter drug or dietary supplement within 2 weeks before screening.

Study Medications and Administration

HPP737 and matching placebo were supplied in capsules containing 1 mg and 5 mg of the active pharmaceutical ingredient. The screening procedure is illustrated in Figure 1. Of 358 screened, 72 were randomized and completed the study as per protocol. In the SAD phase, four sequential cohorts received single doses of 6 mg, 10 mg, 20 mg, or 30 mg. In the MAD phase, two sequential cohorts received either 10 mg or 20 mg once daily for 7 consecutive days. Each dose cohort enrolled 12 participants, with 9 receiving HPP737 and 3 receiving placebo. To ensure standardized conditions, all doses were administered under a unified protocol. Participants fasted for at least 10 hours prior to dosing. The study drug

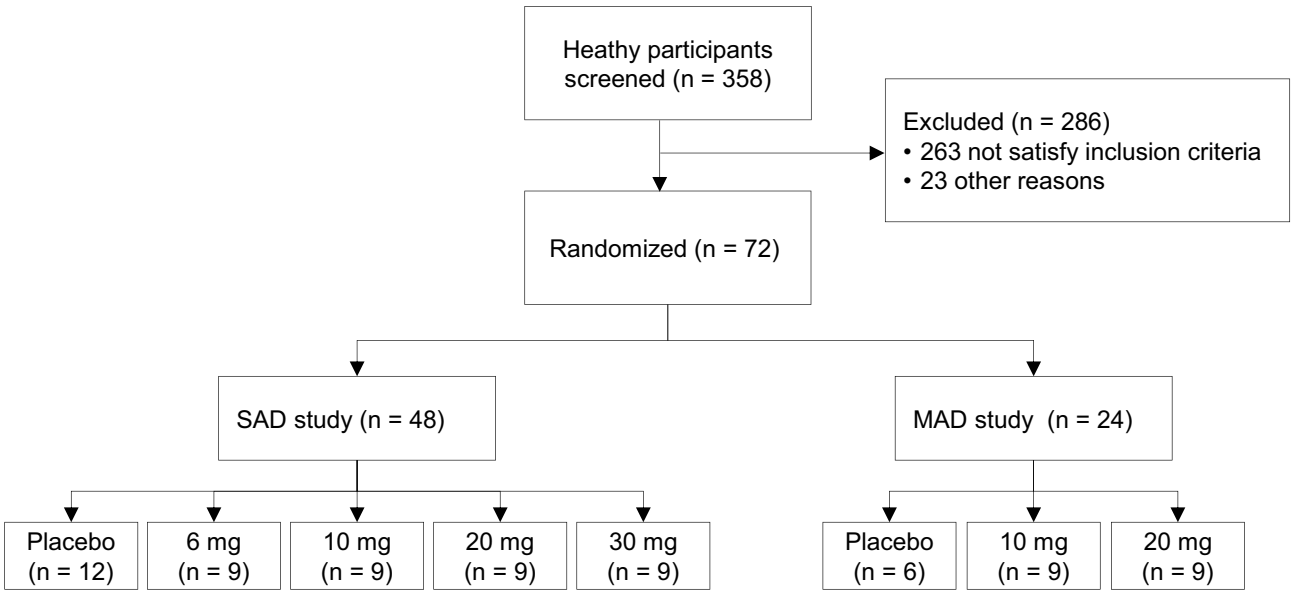

Figure 1 Screening procedure of the study.

https://doi.org/10.2147/DDDT.S598997

was administered within 30 minutes after starting a standardized high-fat, high-calorie breakfast (800–1000 kcal, with approximately 50% of calories derived from fat), followed by 240 mL of warm water. To minimize variability in gastric conditions, no other food or liquid was permitted from 1 hour before until 1 hour after dosing.

Pharmacokinetic Sampling and Bioanalysis

Blood samples for pharmacokinetic analysis were collected at scheduled time points. In the SAD phase, samples were taken pre-dose (0 h) and at 0.5, 1, 1.5, 2, 3, 4, 5, 6, 7, 8, 10, 11, 12, 15, 18, 24, 36, 48, 60, 72, and 96 hours after administration. In the MAD phase, sampling was performed on Day 1 and Day 7 at pre-dose (0 h) and at 0.5, 1, 1.5, 2, 3, 4, 5, 6, 7, 8, 10, 11, 12, 15, 18, 24, 36, 48, 60, and 72 hours post-dose. Additionally, on Day 7 of the MAD phase, samples were also collected at 96 and 168 hours post-dose.

All collected blood samples were centrifuged at 1700 × g and 4°C for 10 minutes to obtain plasma. Plasma concentrations of HPP737 were quantified using a validated liquid chromatography-tandem mass spectrometry method. The assay was linear over the concentration range of 0.1000 to 250.0 ng/mL. Briefly, quantification was performed using an AB Sciex Trap 4000 mass spectrometer coupled with a Shimadzu LC-20AD series liquid chromatography system. Chromatographic separation was achieved on a Thermo Hypersil gold (2.1 × 100 mm, 3 μm) maintained at 40°C, with a mobile phase consisting of (A) 5 mM ammonium acetate solution in water and (B) 0.1% formic acid in acetonitrile. The gradient elution program was as follows: 30% B at 0–0.3 min, increased to 95% B at 0.8 min, held until 1.8 min, then returned to 30% B at 1.81 min and equilibrated until 3 min. The flow rate was 0.7 mL/min and injection volume was 8 μL. Monitoring was performed in positive electrospray ionization mode with the following transitions: m/z 480.0 → 354.0 for HPP737 and m/z 486.3 → 360.0 for the HPP737-d6 (internal standard). The assay demonstrated linearity over the concentration range of 0.1000–250.0 ng/mL ($r^2 > 0.99$). Both intra- and inter-batch accuracy (%bias) and precision (%RSD) met the acceptance criteria. Accuracy was 0.2–13.9% (1.6–17.5% at LLOQ), and precision was ≤7.3% (≤14.6% at LLOQ).

Pharmacokinetics and Statistical Analysis

Noncompartmental analysis (NCA) was conducted using Phoenix WinNonlin software (version 8.3; Certara, Princeton, NJ, USA). The following pharmacokinetic parameters were estimated after single-dose administration: maximum observed plasma concentration (C_{max}), T_{max}, area under the plasma concentration–time curve from time zero to the time of the last measurable concentration (AUC_{0-t}), AUC from time zero extrapolated to infinity (AUC_{0-inf}), percentage of AUC extrapolated ($\%AUC_{ex}$), terminal elimination rate constant (λz), elimination half-life ($T_{1/2}$), apparent oral clearance (CL/F), and apparent volume of distribution (Vd/F). Following multiple-dose administration, the estimated parameters included: time to reach maximum concentration at steady state ($T_{ss,max}$), maximum and minimum plasma concentrations at steady state ($C_{ss,max}$ and $C_{ss,min}$, respectively), average plasma concentration at steady state ($C_{ss,avg}$), AUC_{0-t}, AUC_{0-inf}, $\%AUC_{ex}$, λz,$T_{1/2}$, CL/F, Vd/F, and accumulation ratios.

Statistical analyses were conducted using SAS software (version 9.4; SAS Institute, NC, USA). Descriptive statistics were used for demographic characteristics, pharmacokinetics and safety assessments. Continuous variables with approximately normal distribution are presented as mean ± standard deviation (SD), while non-normally distributed variables (eg., Tmax) are presented as median (range). Categorical variables are presented as number (percentage). For gender-related differences in dose-normalized C_{max} and AUC_{0-24} across dose cohorts, Wilcoxon rank-sum test was employed. This nonparametric method was selected because the small sample size in the female subgroup (n = 2–3 per cohort) precluded reliable assessment of normality and variance homogeneity. The 20 mg multiple-dose group (n = 1 female) was excluded from statistical comparison. Statistical significance was defined as a two-sided P-value < 0.05.

Safety Assessments

All adverse events (AE) were documented and graded according to the National Cancer Institute Common Terminology Criteria for Adverse Events (NCI CTCAE), version 5.0.

Safety assessments, including physical examination, vital signs (blood pressure, pulse, respiratory rate, and body temperature), 12-lead electrocardiogram, and laboratory tests (comprehensive blood biochemistry, complete blood count,

coagulation profile, urinalysis with flow cytometry sediment examination, and pregnancy test), were performed during the screening phase, the treatment phase, and the post-treatment follow-up period.

Results

Demographic Characteristics

The study was conducted from September to December 2022. From an initial pool of 358 healthy Chinese participants, 72 individuals who satisfied all eligibility requirements were selected for enrollment. The demographic and baseline characteristics of all enrolled participants are summarized in Table 1 (SAD phase) and Table 2 (MAD phase). In brief, a total of 48 healthy Chinese participants (Figure 1) were enrolled across four sequential dose cohorts in the SAD phase, with 12 participants per cohort (9 active:3 placebo). The overall population had a mean (SD) age of 25.0 ± 5.2 years (range: 18.0 to 42.0 years), and 79.2% were male. Mean weight, height, and BMI were 67.0 ± 8.6 kg (range: 45.0 to 76.1 kg), 159.6 ± 7.5 cm (range: 145.5 to 181.5 cm), and 21.3 ± 1.4 kg/m^2 (range: 18.9 to 24.2 kg/m^2), respectively. Two participants in the SAD phase (S2001 and S2008) had BMI values slightly outside the protocol-defined range. Upon final eligibility adjudication, it was determined that both participants met all other inclusion requirements and were therefore retained in the full analysis set. In MAD phase, among the 24 healthy Chinese participants (Figure 1) enrolled, 19 were male (79.2%) with a mean age of 28.9 ± 6.5 years (range: 19.0 to 41.0 years). Their mean weight were 61.2 ± 6.7 kg (range: 48.5 to 75.6 kg) with mean height of 167.5 ± 6.5 cm (range: 154.0 to 181.0 cm). Additionally, mean BMI was 21.7 ± 1.1 kg/m^2 (range: 20.0 to 23.5 kg/m^2), which fell within the preset range of protocol. In conclusion, the demographic and baseline characteristics were well-balanced across all dose cohorts.

Table 1 Demographics and Baseline Characteristics in SAD Phase

Characteristics	Placebo (n = 12)	6 mg (n = 9)	10 mg (n = 9)	20 mg (n = 9)	30 mg (n = 9)	Total (n = 48)
Sex, n (%)						
Female, n (%) Men, n (%)	0 (0.0%) 12 (100.0%)	3 (33.3%) 6 (66.7%)	3 (33.3%) 6 (66.7%)	2 (22.2%) 7 (77.8%)	2 (22.2%) 7 (77.8%)	10 (20.8%) 38 (79.2%)
Age, years						
Mean ± SD Median (range)	25.2 ± 3.3 24.0 (21.0–33.0)	24.6 ± 7.4 23.0 (18.0–42.0)	23.6 ± 4.2 22.0 (20.0–34.0)	25.9 ± 4.5 26.0 (19.0–34.0)	25.6 ± 6.8 24.0 (18.0–40.0)	25.0 ± 5.2 24.0 (18.0–42.0)
Body weight, kg						
Mean ± SD Median (range)	62.4 ± 6.7 61.2 (53.6–76.1)	58.3 ± 5.4 56.5 (51.8–67.8)	55.7 ± 7.5 53.9 (45.0–67.5)	62.1 ± 8.6 63.8 (45.5–75.3)	58.3± 8.5 56.0 (46.4–69.5)	59.6 ± 7.5 58.1 (45.0–76.1)
Height, cm						
Mean ± SD Median (range)	170.2 ± 6.7 170.5 (156.0–181.5)	167.4 ± 7.5 170.5 (152.0–175.0)	162.0 ± 8.5 162.0 (145.5–171.0)	168.3 ± 11.4 172.5 (149.0–179.0)	166.2 ± 8.1 166.0 (153.0–178.0)	167.0 ± 8.6 168.3 (145.5–181.5)
Body mass index (BMI), kg/m^2						
Mean ± SD Median (range)	21.5 ± 1.6 20.9 (19.7–24.2*)	20.8 ± 1.4 20.7 (19.1–23.5)	21.2 ± 1.4 21.2 (18.9*–23.4)	21.8 ± 1.3 22.0 (19.9–23.5)	21.0 ± 1.3 20.8 (19.2–23.2)	21.3 ± 1.4 21.0 (18.9*–24.2*)

Notes: *During screening, the BMI values for two participants fell outside the study's reference range. These cases were reviewed and approved for inclusion in the final dataset as exceptions following comprehensive evaluation.
Abbreviations: SAD, single ascending doses; SD, standard deviation.

https://doi.org/10.2147/DDDT.S598997

Table 2 Demographics and Baseline Characteristics in MAD Phase

Characteristics	Placebo (n = 6)	10 mg (n = 9)	20 mg (n = 9)	Total (n = 48)
Sex, n (%)				
Female, n (%) Men, n (%)	2 (33.3%) 4 (66.7%)	2 (22.2%) 7 (77.8%)	1 (11.1%) 8 (88.9%)	5 (20.8%) 19 (79.2%)
Age, years				
Mean (SD) Median (range)	32.3 ± 6.8 32.0 (22.0–41.0)	30.0 ± 4.2 30.0 (25.0–39.0)	25.4 ± 7.1 23.0 (19.0–39.0)	28.9 ± 6.5 28.5 (19.0–41.0)
Body weight, kg				
Mean (SD) Median (range)	63.7 ± 5.7 61.8 (57.3–72.5)	58.6 ± 5.2 58.1 (48.5–67.6)	62.0 ± 8.2 61.8 (51.7–75.6)	61.2 ± 6.7 60.7 (48.5–75.6)
Height, cm				
Mean (SD) Median (range)	169.2 ± 4.7 168.8 (163.5–176.5)	164.1 ± 5.3 166.0 (154.0–170.5)	169.9 ± 7.7 168.5 (158.5–181.0)	167.5 ± 6.5 167.0 (154.0–181.0)
Body mass index (BMI), kg/m^2				
Mean (SD) Median (range)	22.2 ± 0.9 22.1 (21.1–23.3)	21.7 ± 1.2 21.3 (20.4–23.4)	21.4 ± 1.2 21.5 (20.0–23.5)	21.7 ± 1.1 21.5 (20.0–23.5)

Abbreviations: MAD, multiple ascending doses; SD, standard deviation.

Pharmacokinetics Assessment

Figure 2 depicts the mean plasma concentration–time profiles of HPP737 following single oral administrations ranging from 6 to 30 mg (Figure 2A and B), and multiple consecutive daily doses of 10 to 20 mg (Figure 2C and D), administered with a high-fat breakfast to healthy Chinese adults. In SAD phase, as summarized in Table 3, HPP737 exhibited slow absorption, with median T_{max} values ranging from 11 to 15 hours across the dose cohorts. The mean $T_{1/2}$ was approximately 21.2 h, supporting once-daily dosing. The mean Vd/F was calculated to be 209 L, suggesting extensive tissue distribution, while the mean CL/F was 7.4 L/h. After HPP737 administration, interindividual geometric variability for C_{max} ranged from 13.6% to 35.1% in a dose-dependent manner, while for AUC it was consistently higher (>35.5%), suggesting stable total exposure variability despite dose-dependent fluctuations in peak concentration. Both C_{max} and $AUC_{0\text{-}t}$ demonstrated increases in association with higher doses. However, the observed increments were slightly less than dose-proportional. Specifically, the relative mean C_{max} values for the 6, 10, 20, and 30 mg doses were in the ratio 1: 1.3: 2.4: 3.5, and the corresponding $AUC_{0\text{-}t}$ ratios were 1: 1.3: 2.3: 3.2. These observed ratios were lower than the theoretical dose ratios of 1: 1.7: 3.3: 5.0, indicating modest subproportional pharmacokinetics over the tested dose range.

After 7 consecutive days of oral administration with 10 mg or 20 mg HPP737 capsules, the average trough concentrations from days 3 to 14 were comparable. This indicates that steady state was achieved by the third day of dosing. Moderate drug accumulation was observed following continuous dosing. As summarized in Table 4, the accumulation ratios (day 7/day 1) for C_{max} and $AUC_{0\text{-}24}$ were 1.9 and 2.2, respectively, in the 10 mg cohort. Corresponding values in the 20 mg cohort were 1.4 and 1.7, respectively. Notably, pharmacokinetic exposure showed no significant sex-related differences; analysis of C_{max} nor $AUC_{0\text{–}24}$ by dose group and sex revealed comparable values between male and female participants across all cohorts (Figure 3).

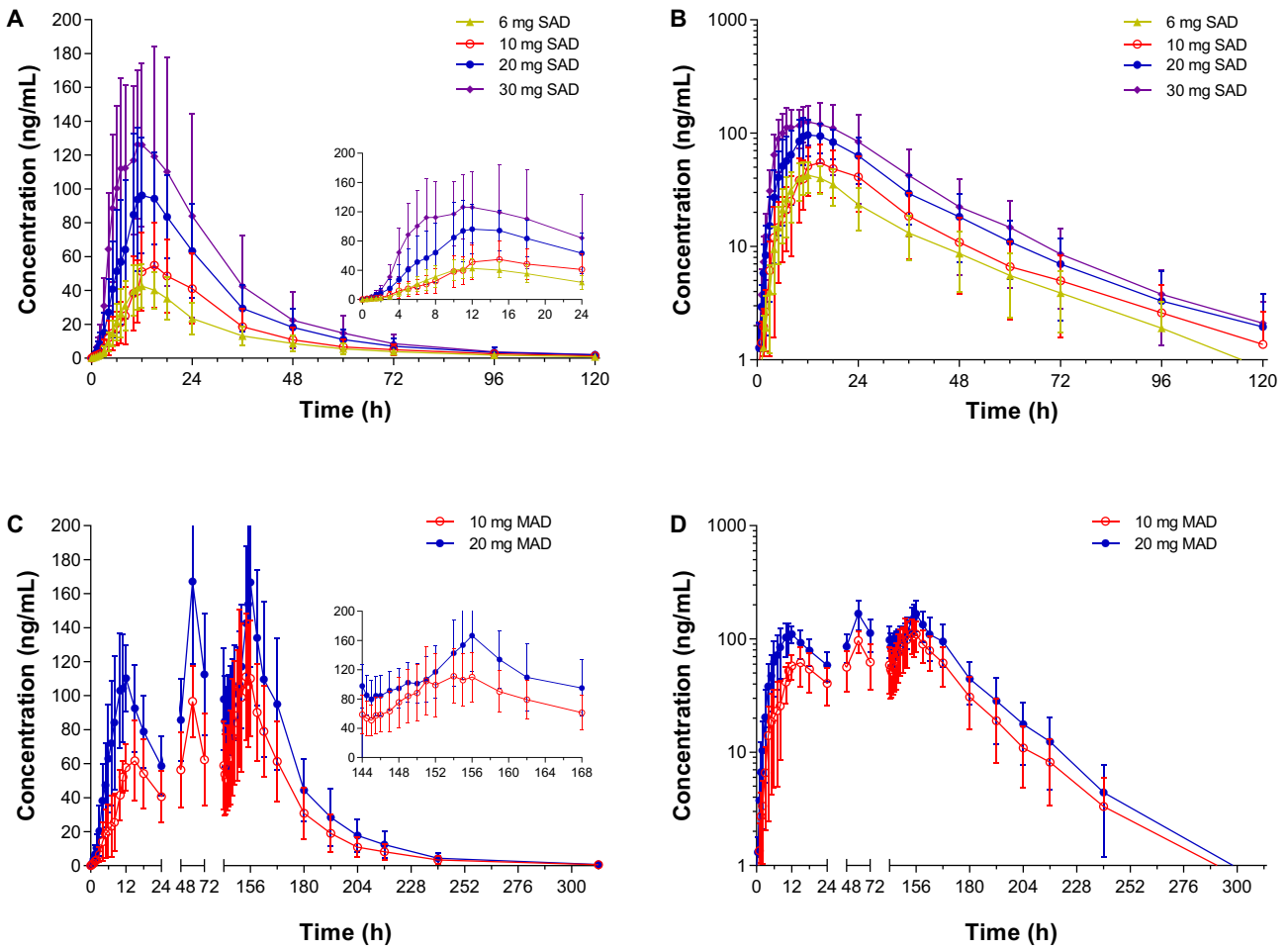

Figure 2 Plasma concentration-time profiles of HPP737 after single and multiple doses. Linear (**A**) and semi-logarithmic (**B**) plots following single ascending doses (SAD). Linear (**C**) and semi-logarithmic (**D**) plots following multiple ascending doses (MAD).
Note: Data was presented as mean ± SD.

Safety Assessments

Treatment-Emergent Adverse Event (TEAEs) were frequently observed, with incidences of 72.9% (35/48) in the SAD phase and 87.5% (21/24) in the MAD phase. Events were predominantly mild (Grade 1) in severity. Two moderate (Grade 2) TEAEs were documented in the SAD phase: asymptomatic hypertriglyceridemia (6 mg cohort) and elevated γ-

Table 3 Pharmacokinetic Parameters of HPP737 After 6–30 mg Single Administration

Parameter (Unit)	6 mg (n = 9)	10 mg (n = 9)	20 mg (n = 9)	30 mg (n = 9)
C_{max} (ng/mL)	50.2 ± 7.1	63.5 ± 23.1	119.5 ± 30.9	174.1 ± 33.8
T_{max} (h)	12 (8–18)	15 (10–24)	11 (6–24)	11 (6–8)
AUC_{0-t} (h*ng/mL)	1237 ± 423	1622 ± 711	2814 ± 910	3897 ± 1672
AUC_{0-inf} (h*ng/mL)	1265 ± 432	1675 ± 756	2902 ± 948	3956 ± 1698
%AUCex (%)	2.3 ± 1.5	2.6 ± 2.9	2.7 ± 4.2	1.4 ± 1.1
$T_{½}$ (h)	21.9 ± 5.7	21.3 ± 10.3	22.1 ± 14.3	19.7 ± 7.0
λz (1/h)	0.034 ± 0.009	0.038 ± 0.015	0.042 ± 0.022	0.039 ± 0.014
CL/F (L/h)	5.3 ± 1.9	7.3 ± 3.7	7.7 ± 2.9	9.2 ± 4.6
Vd/F (L)	174 ± 99	198 ± 79	222 ± 122	243 ± 98

Note: Data are expressed as mean ± SD, except that T_{max} is expressed as median (range).
Abbreviations: C_{max}, maximum drug concentration; T_{max}, time to peak concentration; AUC_{0-t}, area under the plasma concentration–time curve from time zero to the time of the last measurable concentration; AUC_{0-inf}, AUC from time zero extrapolated to infinity; $\%AUC_{ex}$, percentage of AUC extrapolated; $T_{1/2}$, elimination half-life; λz, terminal elimination rate constant; CL/F, apparent oral clearance; Vd/F, apparent volume of distribution.

https://doi.org/10.2147/DDDT.S598997

Table 4 Pharmacokinetic Parameters of HPP737 After Seven consecutive10–20 mg Administration

Parameter (Unit)	10 mg (n = 9)		20 mg (n = 9)	
	Day1	Day7	Day1	Day7
C_{max} (ng/mL)	69.4 ± 18.3	129.7 ± 42.2	121.5 ± 26.0	170.6 ± 45.5
T_{max} (h)	12 (10–15)	8 (6–12)	12 (8–15)	12 (7–15)
$AUC_{0\text{-}24}$(h*ng/mL)	903 ± 211	2000 ± 671	1662 ± 365	2759 ± 790
$AUC_{0\text{-}t}$ (h*ng/mL)	–	3342 ± 1349	–	4755 ± 1719
$AUC_{0\text{-}inf}$ (h*ng/mL)	–	3361 ± 1364	–	4778 ±1730
$\%AUC_{ex}$ (%)	–	0.5 ± 0.4	–	0.5 ± 0.6
$T_{½}$ (h)	–	20.3 ± 5.4	–	21.2 ± 3.3
λz (1/h)	–	0.036 ± 0.010	–	0.033 ± 0.050
CL/F (L/h)	–	5.8 ± 2.8	–	7.8 ± 2.2
Vd/F (L)	–	156 ± 37	–	242 ± 93
$C_{ss,\ min}$ (ng/mL)	–	47.1 ± 19.3	–	73.1 ± 23.0
$C_{ss,\ avg}$ (ng/mL)	–	83.3 ± 28.0	–	114.9 ± 32.9

Notes: Data are expressed as mean ± SD, except that T_{max} is expressed as median (range).
Abbreviations: C_{max}, maximum drug concentration; T_{max}, time to peak concentration; AUC_{0-t}, area under the plasma concentration–time curve from time zero to the time of the last measurable concentration; AUC_{0-inf}, AUC from time zero extrapolated to infinity; $\%AUC_{ex}$, percentage of AUC extrapolated; $T_{1/2}$, elimination half-life; λz, terminal elimination rate constant; CL/F, apparent oral clearance; Vd/F, apparent volume of distribution; $C_{ss,min,}$ minimum plasma concentrations at steady state; $C_{ss,avg}$, average plasma concentration at steady state.

glutamyl transferase (10 mg cohort; follow-up incomplete after day 35). A single severe TEAE (Grade 4), marked by an elevated creatine phosphokinase level (4,870 U/L on day 2), occurred in the placebo group and resolved spontaneously by day 24. No serious adverse events or deaths occurred.

A summary of the most frequent TEAEs (incidence ≥15%) is provided in Table 5 and 6. The overall safety profile comprised laboratory abnormalities (eg., elevated creatine phosphokinase (CPK), ALT, creatinine, triglycerides; proteinuria; hypouricemia), cardiovascular effects (eg., reduced diastolic blood pressure, sinus bradycardia, electrocardiographic T-wave abnormalities), and other common events (eg., chest pain, myalgia).

Notably, hypouricemia occurred exclusively in participants receiving HPP737 capsules, with no cases observed in the placebo group. The incidence was as follows: 2 cases (22.2%) in the single-dose 20 mg group, 2 cases (22.2%) in the single-dose 30 mg group, 1 case (11.1%) in the multiple-dose 10 mg group, and 2 cases (22.2%) in the multiple-dose 20 mg group. Consistent with its pharmacological action, HPP737 administration induced a rapid and dose-dependent reduction in serum uric acid (Figure 4). Furthermore, upon treatment cessation, serum uric acid levels returned to baseline values in all affected participants.

Discussion

This randomized, double-blind, placebo-controlled dose-escalation phase I study in healthy Chinese participants demonstrates that HPP737, a novel PDE4 inhibitor, has a favorable pharmacokinetic and safety profile supportive of its further clinical development for COPD. Brief, the pharmacokinetic profile of HPP737 is distinguished by slow absorption (T_{max}: 11–15 hours), which contrasts sharply with roflumilast (T_{max}: 0.25–2 hours) (see Table 7). Unlike roflumilast, HPP737 has no active metabolite, yet its half-life ($T_{1/2}$ ~21.2 h) is similar to that of roflumilast (19.7–20.9 h). This unique profile supports once-daily dosing with reduced peak-trough fluctuation (6.9 ng/mL vs. 25.0 ng/mL), which may be relevant for tolerability in subsequent studies of COPD.

The single-dose escalation data demonstrate nonlinear pharmacokinetics. As shown in Table 3, increases in systemic exposure (C_{max}, AUC) were less than dose-proportional across the 6–30 mg range, while the elimination $T_1/_2$ remained constant. This profile is mechanistically consistent with saturation of a carrier-mediated uptake process, as suggested by

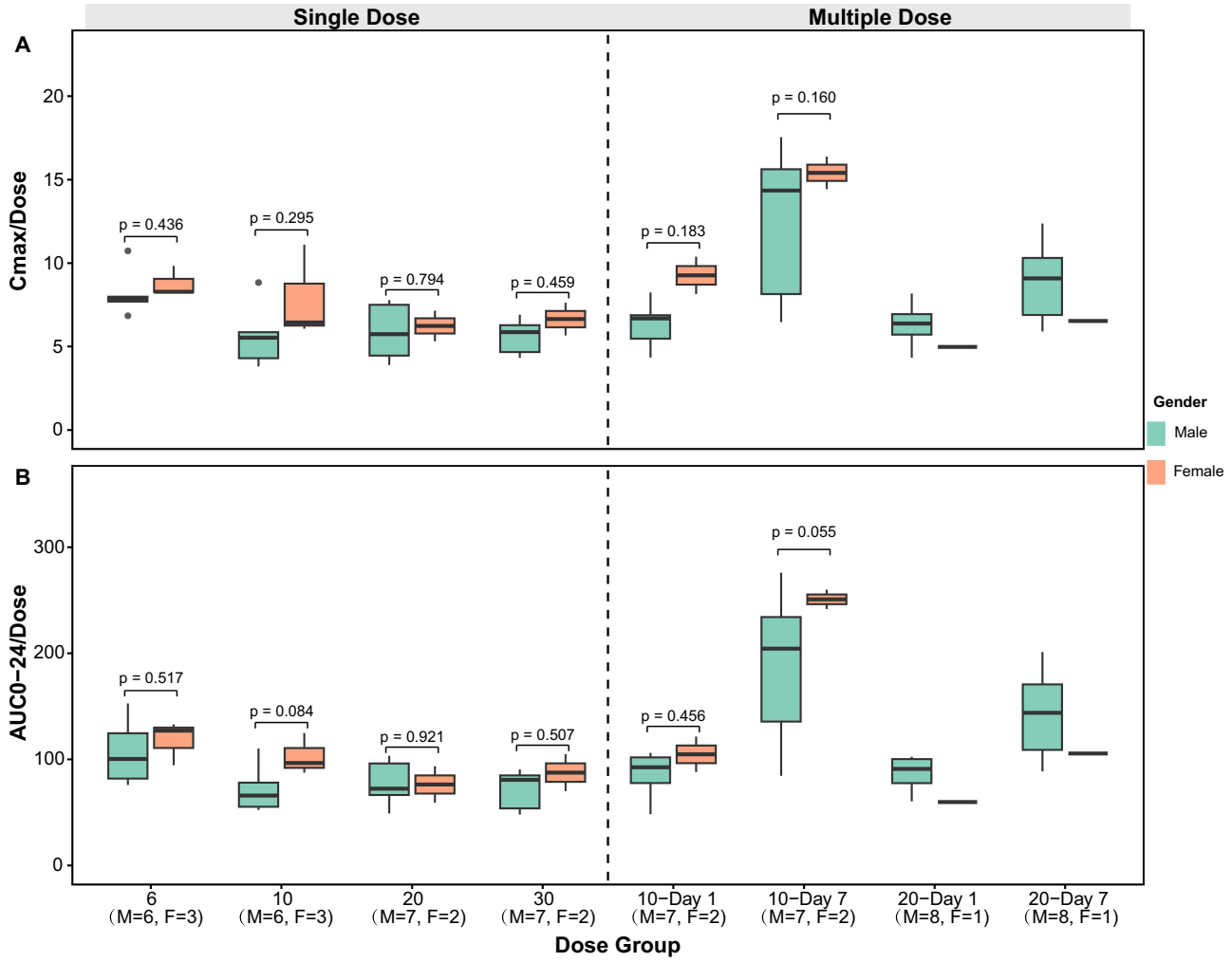

Figure 3 Gender-related differences in dose-normalized C_{max} (**A**) and AUC_{0-24} (**B**) across dose cohorts.
Notes: The 20-mg multiple-dose group (n = 1 female) was excluded from statistical comparison. P <0.05 was considered significant for all tests.

preclinical data. The direct pharmacokinetic manifestation of this saturation is the dose-dependent increase in CL/F and Vd/F—a classic signature of decreasing oral bioavailability (F) at higher doses, as both parameters are inversely related to F.

Based on the food-effect study of HPP737 (Study No: HPP737-101), systemic exposure (AUC)—reflecting PDE4 inhibitory activity[26,27]—was comparable between fasting and postprandial conditions at doses of 3 mg and 12 mg.

Table 5 Most Frequent Treatment-Emergent Adverse Events (TEAEs) Occurring in ≥ 15% of All Participants in SAD Phase

N (%)	Placebo (n = 12)	6 mg (n = 9)	10 mg (n = 9)	20 mg (n = 9)	30 mg (n = 9)	Total (n = 48)
Individuals with any TEAE	8 (66.7%)	7 (77.8%)	7 (77.8%)	5 (55.6%)	8 (88.9%)	35 (72.9%)
DBP decreased	1 (8.3%)	1 (11.1%)	2 (22.2%)	1 (11.1%)	5 (55.6%)	10 (20.8%)
RBC urine positive	0	1 (11.1%)	1 (11.1%)	1 (11.1%)	2 (22.2%)	5 (10.4%)
Heart rate decreased	2 (16.7%)	1 (11.1%)	0	0	2 (22.2%)	5 (10.4%)
T-wave abnormalities	0	2 (22.2%)	1 (11.1%)	2 (22.2%)	0	5 (10.4%)
Urinalysis abnormal (casts)	1 (8.3%)	2 (22.2%)	2 (22.2%)	0	0	5 (10.4%)
BP decreased	0	1 (11.1%)	1 (11.1%)	0	2 (22.2%)	4 (8.3%)
Blood triglycerides increased	0	2 (22.2%)	0	0	0	2 (4.2%)
Sinus bradycardia	2 (16.7%)	1 (11.1%)	0	1 (11.1%)	1 (11.1%)	5 (10.4%)
Hypouricemia	0	0	0	2 (22.2%)	2 (22.2%)	4 (8.3%)
Rash	2 (16.7%)	0	0	0	1 (11.1%)	3 (6.3%)

Abbreviations: SAD, single ascending doses; BP, blood pressure; DBP, diastolic blood pressure; RBC, red blood cells; TEAE, treatment-emergent adverse event.

https://doi.org/10.2147/DDDT.S598997

Table 6 Most Frequent Treatment-Emergent Adverse Events (TEAEs) Occurring in ≥ 15% of All Participants in MAD Phase

N (%)	Placebo (n = 6)	10 mg (n = 9)	20 mg (n = 9)	Total (n = 48)
Individuals with any TEAE	6 (100%)	6 (66.7%)	9 (100%)	21 (87.5%)
RBC urine positive	4 (66.7%)	2 (22.2%)	1 (11.1%)	7 (29.2%)
DBP decreased	0	3 (33.3%)	3 (33.3%)	6 (25.0%)
WBC urine positive	0	2 (22.2%)	1 (11.1%)	3 (12.5%)
T-wave abnormalities	1 (16.7%)	1 (11.1%)	1 (11.1%)	3 (12.5%)
Urinalysis abnormal (protein)	1 (16.7%)	1 (11.1%)	0	2 (8.3%)
Blood CPK increased	1 (16.7%)	1 (11.1%)	0	2 (8.3%)
ALT increased	1 (16.7%)	0	0	1 (4.2%)
Electrocardiogram low voltage	1 (16.7%)	0	0	1 (4.2%)
Blood creatinine increased	1 (16.7%)	0	0	1 (4.2%)
Hypouricemia	0	1 (11.1%)	2 (22.2%)	3 (12.5%)
Sinus bradycardia	0	1 (11.1%)	2 (22.2%)	3 (12.5%)
Chest pain	0	0	3 (33.3%)	3 (12.5%)
Myalgia	0	2 (22.2%)	1 (11.1%)	3 (12.5%)
Constipation	1 (16.7%)	0	0	1 (4.2%)

Abbreviations: MAD, multiple ascending doses; ALT, alanine aminotransferase; CPK, creatine phosphokinase; DBP, diastolic blood pressure; RBC, red blood cells; WBC, white blood cells; TEAE, treatment-emergent adverse event.

However, the average C_{max} was significantly reduced under postprandial conditions. Given the established association between high C_{max} and the incidence of adverse events,[28,29] the postprandial dosing regimen was selected to enhance tolerability while maintaining comparable overall exposure. Consistent with this strategy, our study administered HPP737 postprandially, which likely contributed to the favorable tolerability profile observed.

All adverse reactions were mild or moderate in severity and resolved spontaneously, indicating a favorable safety profile for HPP737. Notably, in contrast to the profile of approved PDE4 inhibitors like roflumilast, both gastrointestinal events (eg., nausea, vomiting), which are specific adverse effects and considered centrally mediated,[22,30] and high incidence of central nervous system-related events (eg., headache, insomnia)[19,22] were infrequent in this study. Only one case of vomiting was reported in the 30 mg dose group. The markedly slower absorption (median T_{max}, 11–15 h for HPP737 vs. approximately 0.25–2.0 h for roflumilast) and the resulting lower peak concentration (dose-normalized C_{max}, 6.9 ng/mL/mg for HPP737 vs. 16.5 ng/mL/mg for roflumilast[20]), as demonstrated in this study, provide a pharmacokinetic basis that is consistent with its preclinical design premise of improved tolerability and aligns with the observed safety profile.

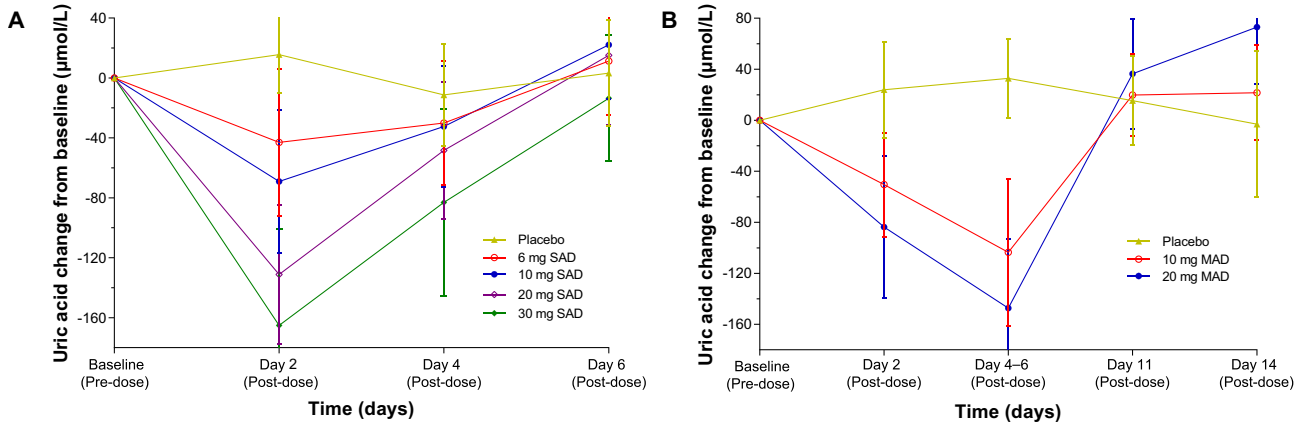

Figure 4 Pharmacodynamic effect of HPP737 on serum uric acid. Mean change from baseline in serum uric acid concentration over time after single ascending doses (**A**) and multiple ascending doses (**B**).
Note: Data was presented as mean ± SD.

https://doi.org/10.2147/DDDT.S598997

Table 7 Comparative Profile of HPP737 versus Roflumilast

PDE4 Inhibitor	HPP737 (Postprandial)	Roflumilast (Fasting)
Primary active entity	Parent drug (HPP737)	Parent drug + active metabolite (roflumilast N-oxide)
C_{max} (ng/mL)*	6.9	Parent: 25.0; metabolite: 29.4
T_{max} (h)	11–15 (slow absorption)	Parent: 0.25–2 (rapid absorption);metabolite: 4.0
$AUC_{0\text{-}24}$ (h*ng/mL)*	90.3	Parent: 95.8; metabolite: 532
Plasma protein binding (%)	90.5	Parent: 99.0; metabolite: 97.0
$T_{1/2}$ (h)	21.2	Parent: 19.7–20.9; metabolite: 23.2–26.2
CL/F (L/h)	5.3–9.2	Parent: 9.5
Vd/F (L)	209 (extensive tissue distribution)	234 (extensive tissue distribution)
Accumulation index	1.4–2.2	Parent: 1.6; metabolite: 3.2
Active metabolite contribution	Not applicable	Metabolite accounts for >90% of total PDE4 inhibitory activity
PDE4 subtype	PDE4B2 and PDE4D2	PDE4B2 and PDE4D2
Metabolite enzyme	Not applicable	CYP1A2 and CYP3A4

Notes: *Represents normalization to 1 mg. Roflumilast data sourced from Huang J et al.[21]
Abbreviations: PDE4, phosphodiesterase 4; C_{max}, maximum drug concentration; T_{max}, time to peak concentration; $AUC_{0\text{–}24}$, area under the plasma concentration–time curve from time zero to 24 hour; $T_{1/2}$, elimination half-life; Vd/F, apparent volume of distribution; CL/F, apparent oral clearance.

A distinct and notable finding was the dose-dependent reduction in serum uric acid (hypouricemia) specific to HPP737 treatment. This effect was reversible and spontaneously alleviated upon treatment cessation. From a pharmacological perspective, PDE4 inhibition by HPP737 reduces the conversion of cAMP to AMP.[31] Given that AMP is a metabolic precursor in the purine catabolism pathway leading to uric acid formation,[29,32] our observation of hypouricemia suggests a likely due to reduced substrate (AMP) availability for uric acid synthesis. While clinically silent in this short-term study of healthy participants, this provides preliminary evidence for a systemic, on-target pharmacodynamic effect. Consequently, serum uric acid might serve as a practical and quantifiable pharmacodynamic biomarker to indicate PDE4 target engagement in future clinical trials, although its validation and the precise mechanistic links require further investigation.

This study has several limitations. First, it was conducted in a relatively small cohort of healthy volunteers, and the enrolled participants were not equally balanced by sex (approximately 79.2% male). However, a post hoc analysis showed no clinically relevant differences in key pharmacokinetic parameters (eg., C_{max} and AUC) between male and female participants. Second, the absolute F of HPP737 has not been established. This parameter should be quantified, and drug-drug interaction studies should be conducted in future trials to fully elucidate the observed exposure differences. Nonetheless, the safety and pharmacokinetics profile in healthy volunteers may not fully predict that in patients with COPD, who are often older and have comorbidities; Finally, the 7-day treatment period was insufficient to assess long-term safety or pharmacodynamic effects. These findings require confirmation in future studies involving patient populations with longer treatment durations.

Conclusion

In conclusion, HPP737 demonstrated a favorable safety and tolerability profile in healthy Chinese participants, supported by its distinct pharmacokinetic characteristics: food-modulated absorption, less than dose-proportional exposure, a long $T_{1/2}$ (~21.2 h), and predictable, moderate accumulation at steady state. These features support once-daily dosing and may provide a pharmacokinetic basis for improved tolerability. A comprehensive understanding of these features is crucial for designing the optimal dosing regimen and formulating clear patient instructions in subsequent clinical trials. The observed dose-dependent reduction in serum uric acid offers a potential pharmacodynamic biomarker for dose optimization. Further studies in patients with COPD are warranted to confirm tolerability, establish the optimal dose, evaluate therapeutic efficacy and explore this biomarker.

Data Sharing Statement

The data that support the findings of this study are available from the corresponding author upon reasonable request.

Ethical Approval

This work was conducted in accordance with the Helsinki Declaration, approved by the Medical Ethics Committee of the Affiliated Hangzhou First People's Hospital, China (2020048-01) and registered at the Chinese Clinical Trial Registry (https://clinicaltrials.gov/; NCT04714294).

Acknowledgments

We thank Newsoara BioPharma and all the participants for their valuable contributions in this study.

Funding

The study was funded by the Construction Fund of Key Medical Disciplines of Hangzhou (Grant number 2025HZZD02) and Key Laboratory of Clinical Cancer Pharmacology and Toxicology Research of Zhejiang Province (Grant number 2020E10021).

Disclosure

The authors declare that they have no competing interests in this work.

References

1. Wang Z, Lin J, Liang L, et al. Global, regional, and national burden of chronic obstructive pulmonary disease and its attributable risk factors from 1990 to 2021: an analysis for the Global Burden of Disease Study 2021. *Respir Res*. 2025;26(1):2. doi:10.1186/s12931-024-03051-2
2. Naeem S, Wang F, Mubarak R, et al. Mapping the Global distribution, risk factors, and temporal trends of COPD incidence and mortality (1990–2021): ecological analysis. *BMC Med*. 2025;23(1). doi:10.1186/s12916-025-04014-0
3. Vollset SE, Ababneh HS, Abate YH, et al. Burden of disease scenarios for 204 countries and territories, 2022–2050: a forecasting analysis for the Global Burden of Disease Study 2021. *Lancet*. 2024;403(10440):2204–2256. doi:10.1016/S0140-6736(24)00685-8
4. Liu M, Wei S, Yang X, et al. Burden of chronic obstructive pulmonary disease and its attributable risk factors in China from 1990 to 2021, with projections to 2050: an analysis of data from the Global Burden of Disease study 2021. *Front Med*. 2025;12:1644022. doi:10.3389/fmed.2025.1644022
5. Yin P, Wu J, Wang L, et al. The burden of COPD in China and its provinces: findings from the Global Burden of Disease Study 2019. *Front Public Health*. 2022;10:859499. doi:10.3389/fpubh.2022.859499
6. Chen S, Kuhn M, Prettner K, et al. The global economic burden of chronic obstructive pulmonary disease for 204 countries and territories in 2020-50: a health-augmented macroeconomic modelling study. *Lancet Glob Health*. 2023;11(8):e1183–e1193. doi:10.1016/S2214-109X(23)00217-6
7. Xu J, Zeng Q, Li S, et al. Inflammation mechanism and research progress of COPD. *Front Immunol*. 2024;15:1404615. doi:10.3389/fimmu.2024.1404615
8. Boswell-Smith V, Spina D, Page CP. Phosphodiesterase inhibitors. *Br J Pharmacol*. 2006;147 Suppl 1:S252-257. doi:10.1038/sj.bjp.0706495
9. Billington CK, Le Jeune IR, Young KW, et al. A major functional role for phosphodiesterase 4D5 in human airway smooth muscle cells. *Am J Respir Cell Mol Biol*. 2008;38(1):1–7. doi:10.1165/rcmb.2007-0171OC
10. Krymskaya VP, Panettieri RA. Phosphodiesterases regulate airway smooth muscle function in health and disease. *Curr Top Dev Biol*. 2007;79:61–74. doi:10.1016/S0070-2153(06)79003-2
11. Wedzicha JA, Calverley PM, Rabe KF. Roflumilast: a review of its use in the treatment of COPD. *Int J Chron Obstruct Pulmon Dis*. 2016;11:81–90. doi:10.2147/COPD.S89849
12. Bateman ED, Rabe KF, Calverley PM, et al. Roflumilast with long-acting β2-agonists for COPD: influence of exacerbation history. *Eur Respir J*. 2011;38(3):553–560. doi:10.1183/09031936.00178710
13. Rennard SI, Sun SX, Tourkodimitris S, et al. Roflumilast and dyspnea in patients with moderate to very severe chronic obstructive pulmonary disease: a pooled analysis of four clinical trials. *Int J Chron Obstruct Pulmon Dis*. 2014;9:657–673. doi:10.2147/COPD.S55738
14. Martinez FJ, Calverley PM, Goehring UM, et al. Effect of roflumilast on exacerbations in patients with severe chronic obstructive pulmonary disease uncontrolled by combination therapy (REACT): a multicentre randomised controlled trial. *Lancet*. 2015;385(9971):857–866. doi:10.1016/S0140-6736(14)62410-7
15. Tashkin DP. Roflumilast: the new orally active, selective phophodiesterase-4 inhibitor, for the treatment of COPD. *Expert Opin Pharmacother*. 2014;15(1):85–96. doi:10.1517/14656566.2013.837159
16. Prickaerts J, Kerckhoffs J, Possemis N, et al. Roflumilast and cognition enhancement: a translational perspective. *Biomed Pharmacother*. 2024;181:117707. doi:10.1016/j.biopha.2024.117707
17. Yuan L, Dai X, Yang M, et al. Potential treatment benefits and safety of roflumilast in COPD: a systematic review and meta-analysis. *Int J Chron Obstruct Pulmon Dis*. 2016;11:1477–1483. doi:10.2147/COPD.S106370
18. Fan T, Wang W, Wang Y, et al. PDE4 inhibitors: potential protective effects in inflammation and vascular diseases. *Front Pharmacol*. 2024;15:1407871. doi:10.3389/fphar.2024.1407871
19. Han M, Lin XY, Cui G, et al. A single-center, open-label, parallel control study comparing the pharmacokinetics and safety of a single oral dose of roflumilast and its active metabolite roflumilast N-oxide in healthy chinese and caucasian volunteers. *Clin Pharmacol Drug Dev*. 2023;12(3):314–323. doi:10.1002/cpdd.1209
20. Li Q, Wang Y, Liu L, et al. Pharmacokinetics of roflumilast and its active metabolite roflumilast N-Oxide in healthy Chinese subjects after single and multiple oral doses. *Eur J Drug Metab Pharmacokinet*. 2017;42(3):371–381. doi:10.1007/s13318-016-0343-4

21. Huang J, Fu CX, Yang XY, et al. Pharmacokinetics of single- and multiple-dose roflumilast: an open-label, three-way crossover study in healthy Chinese volunteers. *Drug Des Devel Ther*. 2018;12:4047–4057. doi:10.2147/DDDT.S178862
22. Rabe KF. Update on roflumilast, a phosphodiesterase 4 inhibitor for the treatment of chronic obstructive pulmonary disease. *Br J Pharmacol*. 2011;163(1):53–67. doi:10.1111/j.1476-5381.2011.01218.x
23. Crocetti L, Floresta G, Cilibrizzi A, et al. An overview of PDE4 inhibitors in clinical trials: 2010 to early 2022. *Molecules*. 2022;27(15). doi:10.3390/molecules27154964
24. Zhang J, Zhai J, Liu H, et al. Phosphodiesterase 4B (PDE4B) inhibitors and their applications in recent years (2014 to early 2025). *Mol Divers*. 2026;30(1):179–195. doi:10.1007/s11030-025-11242-2
25. U.S. Food and Drug Administration. Non-Clinical Review(s) (Application No. NDA 22-522). https://www.accessdata.fda.gov/drugsatfda_docs/nda/2011/022522Orig1s000NonClinR.pdf. Accessed April 20, 2026.
26. Lahu G, Hünnemeyer A, Diletti E, et al. Population pharmacokinetic modelling of roflumilast and roflumilast N-oxide by total phosphodiesterase-4 inhibitory activity and development of a population pharmacodynamic-adverse event model. *Clin Pharmacokinet*. 2010;49(9):589–606. doi:10.2165/11536600-000000000-00000
27. Tenor H, Hatzelmann A, Beume R, et al. Pharmacology, clinical efficacy, and tolerability of phosphodiesterase-4 inhibitors: impact of human pharmacokinetics. *Handb Exp Pharmacol*. 2011;(204):85–119. doi:10.1007/978-3-642-17969-3_3
28. Bethke TD, Böhmer GM, Hermann R, et al. Dose-proportional intraindividual single- and repeated-dose pharmacokinetics of roflumilast, an oral, once-daily phosphodiesterase 4 inhibitor. *J Clin Pharmacol*. 2007;47(1):26–36. doi:10.1177/0091270006294529
29. Jia Q, Yang Z, Wang Q, et al. A liquid chromatography-tandem mass spectrometry method for comprehensive determination of metabolites in the purine pathway of rat plasma and its application in anti-gout effects of Lycium ruthenicum Murr. *J Sep Sci*. 2023;46(21):e2300090. doi:10.1002/jssc.202300090
30. Spina D. Phosphodiesterase-4 inhibitors in the treatment of inflammatory lung disease. *Drugs*. 2003;63(23):2575–2594. doi:10.2165/00003495-200363230-00002
31. Torphy TJ. Phosphodiesterase isozymes: molecular targets for novel antiasthma agents. *Am J Respir Crit Care Med*. 1998;157(2):351–370. doi:10.1164/ajrccm.157.2.9708012
32. Miller SG, Matias C, Hafen PS, et al. Uric acid formation is driven by crosstalk between skeletal muscle and other cell types. *JCI Insight*. 2024;9(2). doi:10.1172/jci.insight.171815